

REPORT DOCUMENTATION PAGE				Form Approved OMB No. 0704-0188	
<small>The public reporting burden for this collection of information is estimated to average 1 hour per response, including the time for reviewing instructions, searching existing data sources, gathering and maintaining the data needed, and completing and reviewing the collection of information. Send comments regarding this burden estimate or any other aspect of this collection of information, including suggestions for reducing the burden, to Department of Defense, Washington Headquarters Services, Directorate for Information Operations and Reports (0704-0188), 1215 Jefferson Davis Highway, Suite 1204, Arlington, VA 22202-4302. Respondents should be aware that notwithstanding any other provision of law, no person shall be subject to any penalty for failing to comply with a collection of information if it does not display a currently valid OMB control number.</small> PLEASE DO NOT RETURN YOUR FORM TO THE ABOVE ADDRESS.					
1. REPORT DATE (DD-MM-YYYY) 07022009		2. REPORT TYPE Journal Article		3. DATES COVERED (From - To)	
4. TITLE AND SUBTITLE Characterization of mud deposit offshore of the Patos lagoon, southern Brazil				5a. CONTRACT NUMBER	
				5b. GRANT NUMBER	
				5c. PROGRAM ELEMENT NUMBER 0601153N	
6. AUTHOR(S) Allen H. Reed, Richard W. Faas, Mead A. Allison, Lauro J. Calliari, K.T. Holland, S.E. O'Reilly, W.C. Vaughan, A. Alves				5d. PROJECT NUMBER	
				5e. TASK NUMBER	
				5f. WORK UNIT NUMBER	
7. PERFORMING ORGANIZATION NAME(S) AND ADDRESS(ES) Naval Research Laboratory Marine Geoacoustics Division Stennis Space Center, MS 39529				8. PERFORMING ORGANIZATION REPORT NUMBER NRL/JA/7430-07-12	
9. SPONSORING/MONITORING AGENCY NAME(S) AND ADDRESS(ES) Office of Naval Research 800 North Quincy Street Arlington VA 22217-5000				10. SPONSOR/MONITOR'S ACRONYM(S) ONR	
				11. SPONSOR/MONITOR'S REPORT NUMBER(S)	
12. DISTRIBUTION/AVAILABILITY STATEMENT Approved for public release; distribution is unlimited					
13. SUPPLEMENTARY NOTES Continental Shelf Research 29 (2009) 597-608					
14. ABSTRACT Rapid deposition of mud on the beach along the shoreface of Rio Grande do Sul, Brazil dramatically influences the normal operations in the littoral zone. In the surf zone, fluid and suspended mud opposes water-wave movement and dissipates water-wave energy; on the beach, mud limits trafficability. As part of a multinational, multidisciplinary program to evaluate the influence of mud strength, density and viscosity on water-wave attenuation, sediments were evaluated in situ or collected for evaluation from an area offshore of Cassino Beach, slightly south of the Patos Lagoon mouth. Shear strength of deposited sediments ranged from 0.6 kPa at the seafloor to 3.4 kPa at ~1 m below the seafloor. Mud sediments were also collected to simulate the in situ response of fluid mud to shear stresses. For this determination, rheological evaluations were made using a strain-controlled Couette viscometer on numerous remixed samples that ranged in density from 1.05 to 1.30 g/cm ³ . It was determined that this mud is a non-ideal Bingham material in that it has a true initial yield stress as well as a upper Bingham					
15. SUBJECT TERMS Fluid mud, Sediment strength, Geochronology, Rheology, Viscosity					
16. SECURITY CLASSIFICATION OF:			17. LIMITATION OF ABSTRACT UU	18. NUMBER OF PAGES 12	19a. NAME OF RESPONSIBLE PERSON Allen Reed
a. REPORT Unclassified	b. ABSTRACT Unclassified	c. THIS PAGE Unclassified			19b. TELEPHONE NUMBER (Include area code) 202-688-5473

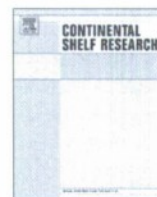
20090515192



ELSEVIER

Contents lists available at ScienceDirect

Continental Shelf Research

journal homepage: www.elsevier.com/locate/csr

Characterization of a mud deposit offshore of the Patos Lagoon, southern Brazil

Allen H. Reed^{a,*}, Richard W. Faas^b, Mead A. Allison^c, Lauro J. Calliari^d, K.T. Holland^a, S.E. O'Reilly^e, W.C. Vaughan^e, A. Alves^d

^a Naval Research Laboratory, SSC, MS 39529, USA

^b Department of Marine Sciences, University of Southern Mississippi, SSC, MS 39529, USA

^c Institute for Geophysics, University of Texas, Austin, TX 78758-4445, USA

^d Fundação Universidade da Rio Grande, Brazil

^e Minerals Management Service, New Orleans, LA 70112, USA

ARTICLE INFO

Article history:

Accepted 5 February 2009

Available online 7 February 2009

Keywords:

Fluid mud

Sediment strength

Geochronology

Rheology

Viscosity

ABSTRACT

Rapid deposition of mud on the beach along the shoreface of Rio Grande do Sul, Brazil dramatically influences the normal operations in the littoral zone. In the surf zone, fluid and suspended mud opposes water-wave movement and dissipates water-wave energy; on the beach, mud limits trafficability. As part of a multinational, multidisciplinary program to evaluate the influence of mud strength, density and viscosity on water-wave attenuation, sediments were evaluated in situ or collected for evaluation from an area offshore of Cassino Beach, slightly south of the Patos Lagoon mouth. Shear strength of deposited sediments ranged from 0.6 kPa at the seafloor to 3.4 kPa at ~1 m below the seafloor. Mud sediments were also collected to simulate the in situ response of fluid mud to shear stresses. For this determination, rheological evaluations were made using a strain-controlled Couette viscometer on numerous remixed samples that ranged in density from 1.05 to 1.30 g/cm³. It was determined that this mud is a non-ideal Bingham material in that it has a true initial yield stress as well as an upper Bingham yield stress. Initial yield stress ranged from 0.59 to 2.62 Pa, upper Bingham yield stress ranged from 1.05 to 7.6 Pa. Apparent viscosity ranged from 0.02 to 4.7 Pa s with the highest viscosities occurring between the two yield stresses. Sediment strength in the remixed samples is 2 to 3 orders of magnitude lower than the horizontal shear strength of the sediment bed as determined by shear vane or predicted from penetrometer measurements. This difference is partially due to the fact that rheological evaluations are made on fully remixed sediments, whereas horizontal shear strength is determined within relatively undisturbed sediments. Similar values of viscosity and shear strength are comparable to those determined for mud in other coastal areas where fluid mud deposits occur.

© 2009 Elsevier Ltd. All rights reserved.

1. Introduction

The southern-most beach in Brazil provides a roadway along a surfing area between the mouth of the Patos Lagoon and Uruguay, at least most of the time. Episodically, mud is transported from an offshore deposit through the surf zone and onto the beach as was the case in 1999, 2004 and 2007. As mud enters into the littoral zone and onto the beach, the mud dissipates wave energy and if transported onto the beach, the mud limits pedestrian, cart and automobile traffic. To determine the sediment properties in this area and the potential interaction between mud and water waves, a multinational group of scientists studied the physics of

mud–wave interactions by measuring properties of the mud, the characteristics of the waves and modeling the potential interaction between the two. This paper focuses on the mud properties, specifically sediment strength and rheological behavior, of a nearshore deposit adjacent Cassino Beach.

The geotechnical properties of this mud deposit are similar to coastal mud deposits in many other areas where mud strength, viscosity and density have worked to dissipate wave energy (Calliari and Fachin, 1993; Holland et al., 2007, Fig. 1; Dias and Alves, 2007). Examples of such coastal mud deposits occur off of Kerala, India (Jiang and Mehta, 1996; Mathew et al., 1995), the Amazon River, central and southern regions of Brazil (Kineke and Sternberg, 1995; Gabioux et al., 2005), Surinam, Guyana, and Venezuela (Wells and Coleman, 1981; Allison and Lee, 2004; Winterwerp et al., 2007), England (Ingliss and Allen, 1957), and the Atchafalaya Basin, Southern Louisiana, USA (Sheremet et al.,

* Corresponding author. Tel.: +1 228 688 5473.

E-mail address: allen.reed@nrlssc.navy.mil (A.H. Reed).

2005; Allison et al., 2000; Fan et al., 2004; Jiang and Mehta, 1996). In these areas, the mud deposit is typically comprised of a fluid mud layer that overlies a consolidated mud deposit. The fluid mud tends to be a well-mixed flocculated suspension of varied water content within which the sediment strength is isotropic. The consolidated mud deposit is denser, dewatered to a larger extent, and has anisotropic strength due to such things as bioturbation and stratigraphy layers. Both the fluid and the consolidated mud may respond elastically to applied stress, but both will deform plastically after a critical shear stress is reached. It has been generally determined that fluid mud may dissipate up to 90% of the wave energy, therefore based upon the scope of this project, the properties and behavior of the fluid mud are viewed as more important than the properties of the consolidated mud.

Fluid mud may, however, be difficult to define and isolate in the seafloor, but it can be determined by geotechnical behavior or response of the mud to stress and strain and bulk density of the deposit. That is fluid mud is a high-density suspension of fine grained particulates that behaves as a viscous fluid. Generally, sediment concentration within a fluid mud has been found to range from 10 to 480 g per liter of water, which corresponds to a density of approximately $1.05\text{--}1.30\text{ g/cm}^3$ (Ingliss and Allen, 1957; Wells and Coleman, 1984). Fluid mud is appropriately defined by geotechnical behavior, specifically its response to strain or shear stress. It has been determined to be a non-Newtonian, shear thinning or thixotropic fluid that may behave in two distinct ways depending upon the applied stress or shear rate (Nguyen and Boger, 1992, Fig. 9; Barnes, 1999; Mehta, 1989; Faas, 1991; Toorman, 1994). Mud within this density range may behave as a viscoelastic suspension of dispersed particles with limited particle interaction that is created during grain settling. Within a short time after settling to the seafloor, perhaps within 10 min to 24 h of settling, depending upon the stresses imposed upon it, the sediment assumes a gelled state, which may behave as a viscoelastic fluid which can reclaim its former state after a stress is applied. If the critical stress for deformation is exceeded, that is after a critical yield stress is exceeded, fluid mud behaves as a viscoplastic material in which the initial state of the fluid mud is not recoverable.

Rheological measurements are commonly made to determine the critical yield stress, to evaluate fluid mud behavior and to determine viscosity (Faas, 1991; Toorman, 1994). To create fluid mud, samples are remixed so that the binding forces imparted by physico-chemical bonds to adjacent grains are broken, which results in a fully remolded and relatively weak sediment slurry. The remixed sediment is often evaluated with a strain-controlled Couette viscometer, such as the Brookfield RVT (Williams, 1979). Stresses are applied to the remixed muds of varied densities at incremental strains and stress is calculated from a dial reading to enable viscosity to be quantified and behavior to be determined. The viscosity data that is determined for specific mud densities may then be incorporated directly into numerical models, such as SWAN, to predict the dissipation of wave energy (Rogers and Holland, this issue; Winterwerp et al., 2007). Rheological measurements are also vital to in other wave models that predict the relationship between fluid mud strength, viscous behavior and damping of water waves (Gade, 1958; Dalrymple and Liu, 1978; Isobe et al., 1992; Feng, 1992; Faas, 1995; Shibayama et al., 1986; MacPherson, 1980; Maa and Mehta, 1987, 1989; Jiang and Mehta, 1996; Nguyen and Boger, 1992; Mei and Liu, 1987; Tsuruya et al., 1987).

Within these wave-damping models, several factors come in to play on how the rheological behavior of sediments should be incorporated and addressed. Numerous rheological models have been invoked to address the non-linear viscous response of fluid muds (e.g., Casson, Herschel–Bulkley, Bingham, etc.). These

models are based on factors such as initial yield stress, Bingham yield stress, and viscosity and they may have several variables or factors that need to be computed to plot the stress–strain data, therefore the efficacy of using such models may be questioned (Nguyen and Boger, 1992; Toorman, 1994). For instance the Bingham model assumes that the initial yield stress and the Bingham yield stress are one and the same and that a linear relationship between stress and strain occurs after the Bingham yield stress is exceeded, whereas the Herschel–Bulkley model assumes a non-linear, power law relationship between stress and strain after the initial yield stress is exceeded. Additional variables are also required for the Herschel–Bulkley model. In cases where these fluid mud models are not applicable to the stress–strain behavior of the fluid mud, another option is possible, that is the fluid mud may be addressed as a non-ideal fluid that does not exactly fit a specific model (Krieger and Maron, 1954). In fact, in some fairly recent work, it was determined that the mud exhibited a non-ideal Bingham behavior, possessing an initial yield stress that occurred prior to the Bingham yield stress, such that highest mud viscosity occurred between an initial yield stress and the “upper” Bingham yield stress (Nguyen and Boger, 1992, see Fig. 9; Toorman, 1994). In these cases, the initial yield stress is the first deformation of the sediment and the “upper” Bingham yield stress is determined by extrapolating to the stress axis from the linear portion of a stress–strain curve.

When remixed sediments are isolated from shear stresses or strains, they alter from low strength, low-density muds to higher strength deposits provided as the sediment dewater, consolidates and establish physico-chemical bonds that impart strength increase intergranular cohesiveness. For this to occur, sediments need to be isolated from critical shear stresses that would otherwise retain the sediment as a low-density suspension. The rate at which this occurs determines the rate at which a recent deposit assumes increased strength. Geochronology provides a means to determine sediment accumulation rates and the amount of time that sediments have been retained on the seafloor and isolated from critical shear stresses that would remobilize them and allowed to dewater. Sediment accumulation rates are determined by making laboratory measurements of radioactive decay for specific radioisotopes (^{234}Th , ^7Be , ^{137}Cs , ^{210}Pb) that have adsorbed onto the surfaces of particles, particularly highly reactive surfaces such as those of clay minerals. Because the decay rate (i.e., activity) for these isotopes varies, the sediment accumulation rate can be determined over periods ranging from months (^{234}Th , ^7Be) to decades (^{137}Cs , ^{210}Pb) thereby making it possible to determine sediment stability and accumulation rates over years to centuries. An additional benefit of these analyses is that radioisotopes have differences in source functions (e.g., U-series decay, cosmogenic, bomb-produced), therefore activities of specific radiotracers in surficial sediments can be indicative of sediment source. Specifically, ^7Be and ^{137}Cs tend to be higher in riverine or nearshore sediments and indicate a nearshore sediment source, whereas ^{234}Th is more prevalent in offshore sediments exposed to water enriched in dissolved U (Allison et al., 2000).

Rapid accumulation rates work to inhibit release of interstitial water, which inhibits the increase in sediment strength. Correlations between sediment water content (i.e., density) and sediment strength have been made for Atterberg limits, which are commonly used to compare geotechnical properties of muds from different regions (Faas, 1991). The two limits most important in these determinations are the liquid limit, which is the boundary between fluid and plastic behavior and the plastic limit, which is the upper limit for plastic behavior. At the liquid limit, mud strength has been found to be $\sim 1.7\text{--}2.5\text{ kPa}$, which is approximately the shear strength (determined by vane shear on

undisturbed samples that are not remixed) of some shallowly deposited muddy sediments located along the Kerala Coast of India, the Baltic Sea, the Gulf of Mexico and elsewhere (Silva et al., 1996; Narayana et al., 2008). At the plastic limit, the relatively dry sediment is highly consolidated, prone to fracture and has shear strength that is ~ 170 kPa (Mitchell, 1976; Wroth and Wood, 1978). Sediments that are deposited to the seafloor and are isolated from stress tend to be at or above the strength correlated to the liquid limit.

In addition to temporal controls on sediment strength, there are numerous other factors that influence and influence strength of fluid and consolidated mud deposit (e.g., mineralogy, silt:clay ratio, colloid concentration, temperature, stress-strain history), however these have not been addressed in this paper. Rather this paper characterizes the mud deposit adjacent to Cassino Beach in terms of offshore continuity, depositional history, sediment strength and rheological behavior in order to provide parameters and domain information to numerical models that will model wave energy dissipation in the Cassino Beach area. Therefore the following determinations were made. First, the offshore continuity of the mud deposit was made as it determines the fetch over which surface water waves may interact with the mud deposit. Second, the depositional history or accumulation rate was determined at within the heart of the mud depocenter and to the south of this location. Third, the sediment strength is determined from shear strength and bearing strength measurements. Fourth, fluid mud response to increasing shear rate was determined using a strain-controlled Couette viscometer on sediment samples that were remixed to varied densities associated with fluid mud.

2. Study site and methods

2.1. The site

The Patos Lagoon, located in southern Brazil, is the largest estuary in South America. It extends from the lagoon mouth, adjacent to the town of Cassino Beach in Rio Grande do Sul, 190 km north to the city of Porto Alegre. The lagoon has a width of ~ 64 km and approximately 10,100 square kilometers of surface area. Below the lagoon lies one of South America's largest coastal aquifers, which discharges $\sim 980 \text{ m}^3 \text{ s}^{-1}$ of ground water into coastal waters (Niencheski et al., 2007). More importantly, the lagoon provides the primary link between the ocean and five rivers (e.g., Guaíba, Camaquã and others) which supply a mean inflow of $2000 \text{ m}^3 \text{ s}^{-1}$ and a maximum inflow reaching $5000 \text{ m}^3 \text{ s}^{-1}$ during El Niño events (Fernandes et al., 2002).

The suspended sediments that are transported through the lagoon mouth flow out of the lagoon in a southeasterly direction with some of these sediments maintained in a clockwise flow that carries them westward toward the coast near Querência, and northward towards Cassino Beach where a primary depositional area has been determined (Calliari and Fachin, 1993; Vinzon et al., this issue; Holland et al., 2007).

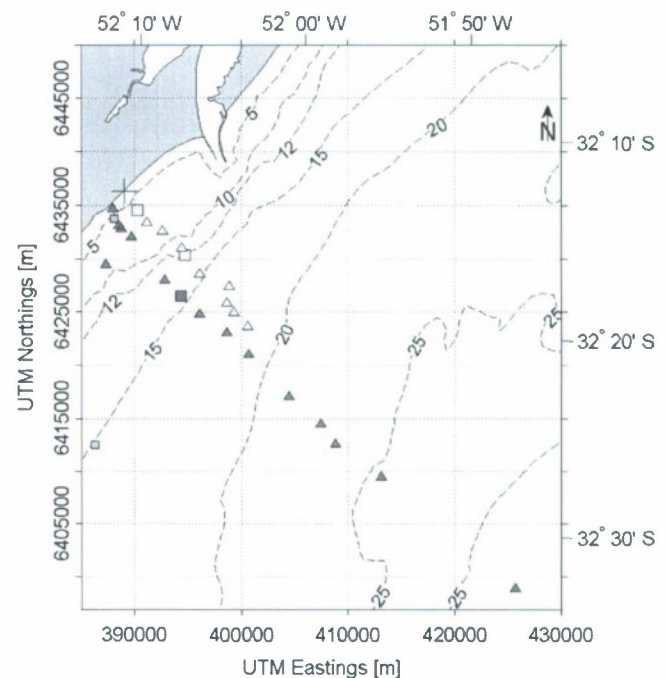
During the Cassino experiment in 2005, a sensor transect was established shoreward and offshore of the Fundação Universidade do Rio Grande biological/fisheries research station in Querência to monitor the wave regime across the mud deposit (Holland et al., 2007). The mud depocenter and areal extent of the mud appears to be ephemeral, however observations have shown that the mud deposit oscillates around the vicinity of the sensor transect and extends from nearshore to offshore, near the 25 m isobath. In the vicinity of this transect, a significant volume of mud may be transported through the surf zone and onto the beach as was the case when mud was deposited on shore in 2004, prior to the 2005 experiments and in 2006 prior to our November 2006 cruise and

again in December 2007. Episodic transport of fluid mud through the surf zone and onto the beach provides impetus for continued evaluations in this area.

2.2. Sampling and cruises

Three sampling cruises were conducted to evaluate mud in the area of the Querência Transect that was established in 2005 (Holland et al., 2007; Fig. 1). The first cruise was in May 2005 aboard the *Cassino 8* trawler, the second was in November 2006 aboard the *R/V Larus* and the third was in October 2007 aboard the *Ru Chu*. The purpose of these cruises was to collect bottom sediment samples to determine sediment rheology, shear strength, accumulation rates and grain size and to measure sediment bearing strength in situ.

During the 2005 cruise aboard the *Cassino 8*, divers collected cores from 14 and 15 m water depth (Fig. 1). These cores were subsampled at 5 cm intervals for geochronological analysis (^{7}Be , ^{137}Cs , ^{210}Pb) and grain size. Bearing strength was also measured at the 15 m depth using a lance penetrometer. During the 2006 cruise, aboard the *R/V Larus*, grab samples were collected with a Van Dorn sampler at 14 stations along the same transect. The grab samples were used to determine grain size, rheological properties for established sediment densities. Divers collected 6 cm diameter core samples at selected stations and these were used to quantify sediment accumulation rates and determine whether physical or biological processes dominate sediment mixing. During the 2007 cruise, SCUBA divers collected cores at 2 different sites to determine shear strength by shear vane tests, so that correlations between sediment shear strength and bearing strength (normal incidence shear strength) could be established and verified for this area, thereby establishing a realistic factor by which to predict horizontal shear strengths from normal



incidence shear strength determined from penetrometer deployments.

Rheological behavior and apparent viscosity were determined using a Brookfield RVT rotational viscometer at The University of Southern Mississippi (USM). Shear strength from vane tests was determined at Fundação Universidade do Rio Grande (FURG). Sediment accumulation rates were determined at Tulane University (Tulane) using a Canberra Germanium detector. Grain size was determined from grab samples and diver-collected cores at FURG and at the Naval Research Laboratory (NRL).

2.3. Rheology: mud behavior and classification

Rheological determinations were made on mud that was obtained from surface grab samples during 2006. The samples were remixed and density was adjusted with seawater of comparable salinity to what was measured in the area of the Querência Transect. The samples were well-mixed prior to evaluation by a strain controlled, Brookfield RVT rotational viscometer.

Our specific goals were to determine the strength and behavior of the fluid mud, which had been remixed to obtain consistent slurry with a density in the range $1.05\text{--}1.30\text{ g/cm}^3$. Fluid mud strength was determined prior to, during and after the initial deformation was obtained, such that determinations were made after increasing strains were applied. Thereby, this data provides a determination of viscosity and behavior of the fluid mud that was remixed to varied densities.

Couette viscometers are commonly used to determine rheology of Newtonian fluids, where the relationship between shear stress and shear rate is linear and the apparent viscosity is constant. These viscometers are also successfully used to accurately determine strength and behavior of non-Newtonian fluid suspensions, such as fluid mud, by supplying corrections to the manufacturer's protocol (see Rosen, 1979, p. 32ff; Krieger and Maron, 1954; Barnes, 1999).

To make determinations of the fluid mud properties, we used an 8-speed, strain-controlled, Brookfield RVT rotational viscometer that is equipped with a couette-type cup and bob system with a narrow gap (1.24 mm) UL Adapter. The internal diameter of the viscometer cup is 27.62 mm and external diameter of the viscometer bob is 25.15 mm; the ratio between the two is 1.098. Sediment samples were prepared by hindered settling of a fully dispersed sample of wet sediment ($\sim 50\text{ g}$ (dry wt)) in a 1 l settling tube filled with water that had a salinity of 32 ppt. After 20–24 h, the sediment had settled from the top portion of the cylinder, the clear water was decanted and four subsamples of increasing density were carefully poured from the settling tube into small containers. From these containers, a sample was carefully poured into the viscometer cup, the viscometer bob was inserted into the cup and submerged in the mud and the entire apparatus was attached to the viscometer. The viscometer was leveled, so that the bob was vertically aligned in the cup, and rotation of the bob was initiated at the lowest rpm (0.5). The dial that records deflection was zeroed prior to each analysis. During the initial analysis run, at the lowest shear rate (0.5 rpm), dial recordings were made for an initially high value and a lower, stable value where the dial remained during the rest of the initial analysis run. The high value or maximum dial reading obtained at the lowest shear rate (0.5 rpm) provides the basis for determining the initial yield stress. For each shear rate, dial readings were made and recorded after the dial had stabilized. This was done successively for subsequent analysis runs that were conducted at varied shear rates (1.0, 2.5, 5.0, 10.0, 20.0, 50.0 and 100 rpms). After the 100 rpm reading was recorded, the sequence was reversed. A single ascending–descending cycle took $\sim 25\text{ min}$. Once the

measurements were completed, the sample slurry was poured into a pre-weighed container, reweighed, and placed in a 105°C drying oven. After 24 h, the sample was removed from the oven and reweighed. The water content (% dry wt), % volume, and bulk (wet) density (corrected for salt content) were determined.

Rheological shear stress is determined by multiplying the recorded dial reading (i.e., shear stress on the bob) by the spring constant divided by the radius and the effective length of the bob. Shear strain rates are corrected for each rpm using a computational method formulated by Krieger and Maron (1954) and truncated by Rosen (1979) so the shear stress at the bob is properly determined and samples that contained slippage can be determined and left out of the interpretation. Apparent viscosity is then determined as the ratio of the corrected shear stress to the shear rate.

The initial (static) yield stress is the stress at which the mud first deforms and 'upper' Bingham yield stress is the stress extrapolated from the second yield, which is demarcated by an inflexion in the curve on the stress–strain plot. Specifically, the initial (static) yield stress is determined as the maximum shear stress and maximum dial reading that is attained at the lowest (0.5 s^{-1}) shear strain rate. The Bingham yield stress is determined as value at the intersection with the y-axis of a line extrapolated from the linear portion of the stress–strain curve that is obtained for the higher strain values (Fig. 2). From here on, initial (static) yield stress is referred to as initial yield and 'upper' Bingham yield stress is referred to as Bingham yield stress.

By plotting shear stress to shear strain rate, the nature and viscosity of the flow behavior is determined on a flow-diagram. Pseudoplastic or shear-thinning behavior is commonly determined for muds. Graphically, this behavior is evidenced as a decrease in shear stress with subsequent increases in shear strain. This can be compared with other plots of sediment strength versus shear rate, such as non-Newtonian dilatant or shear thickening behavior in which sediment strength increases with increasing shear rate or with Newtonian behavior in which the ratio of sediment strength to shear rate remains constant for all shear stresses or shear rates.

2.4. Shear strength

Normal incidence shear strength or bearing strength was determined using a lance penetrometer, STING MKII, from three successive deployments per station. The configuration of the penetrometer was a 2-m-long shaft with a 70-mm-diameter foot (Fig. 3), which has been correlated to shear strength on numerous occasions (Abelev, 2008). The penetrometer is deployed by hand, lowered over the side of the boat and into the water and then allowed to free fall to the sediment which it penetrates until it comes to a stop.

In each deployment, acceleration and pressure changes are recorded at 0.5 s intervals. The acceleration data are then converted to bearing strength by accounting for the drag forces acting on the penetrometer and computing the force exerted by the sediment upon the penetrometer. The bearing strength is calculated as the force per unit area of the foot (38.5 cm^2) divided by the strain rate, which is equivalent to the 0.15 power of the inverse of time that it takes to penetrate the mud a distance equal to the foot diameter (i.e., 70 mm) (Preston et al., 1999).

The usefulness of this device is two fold. First, the penetrometer enables a determination of the sediment strength through the vertical bedding over the depth of penetration. This will provide some indication of the mud thickness in specific areas. Second, the penetrometer provides a means to indirectly predict horizontal shear strength with depth. This results because correlations

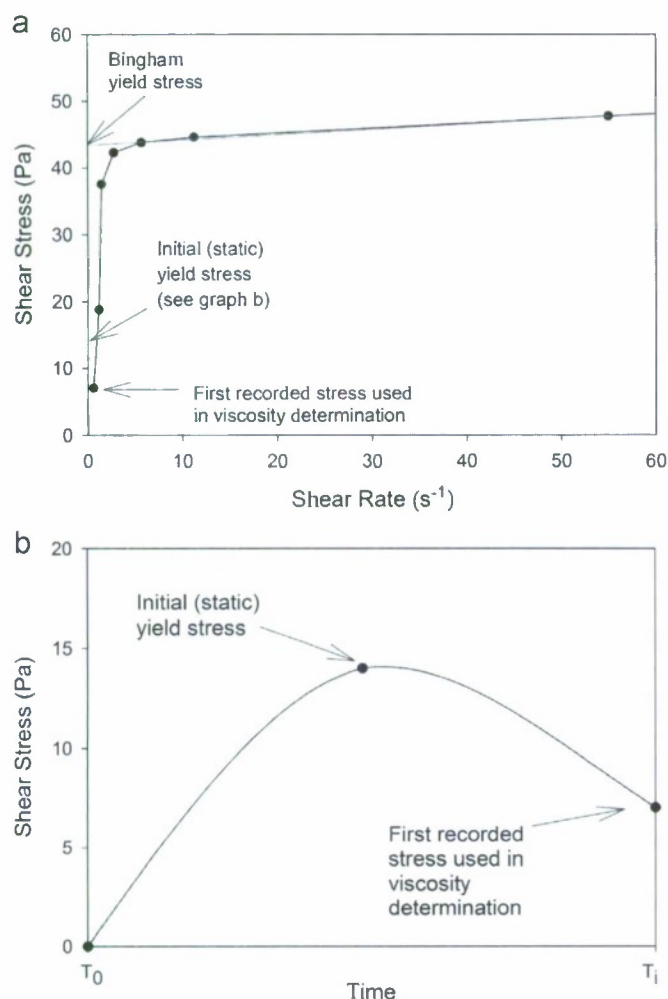


Fig. 2. (a) Bingham yield stress is determined at the intersection between a line that is extrapolated from the straight line portion of a shear stress versus shear rate plot to the y-axis. This curve is based upon rate corrected values for Que. 8, which had a density of $1.196 g/cm^3$. The initial (static) yield stress is the first recording made during a viscometric evaluation. It is larger than the value used in determination of viscosity (shear stress/shear rate). (b) Cartoon illustrating the determination of initial (static) yield stress. Initial yield stress is determined as the maximum dial reading which occurs between the beginning (T_0) and the end (T_1) of the first shear rate (0.61 revolutions/s) evaluation.



Fig. 3. The STING MKII penetrometer is a hand-deployed and tethered instrument measures acceleration and pressure and predicts bearing strength.

between shear vane measurements (horizontal shear strength) and bearing strength (normal incidence shear strength) have been established on soft sediment deposits that have similar strengths of Cassino Beach muds. The best correlations for a wide array of sediments is that bearing strength is 10 times the horizontal shear strength as measured on cores with a shear vane (Preston et al., 1999; Mulhearn, 2003). The validity of this correlation is substantiated by shear vane measurements made at FURG on diver-collected cores, which were collected in 2007.

Horizontal shear strength was determined from shear vane measurements made in the laboratory on 6 cm diameter diver-collected cores using a shear vane manufactured by Viatest GmbH.

This shear vane is comprised of four blades that are oriented vertically and perpendicular to the shaft at 90° intervals. Each blade is 12.7 mm long by 12.7 mm wide. These blades rotate at a set rate to apply stress to the mud along horizontal planes until the sediment fails. At this point a dial reading is recorded. Horizontal shear strength is determined from the dial reading and the spring calibration factor in accordance with the Viatest GmbH's recommendations.

It is necessary to note that while bearing strength is a determination of the average normal contact stress between an object and the sediment that will result in failure or normal yielding of the sediment, horizontal shear strength, as determined by a shear vane, is the maximum sediment strength mobilized in a cylindrical surface with an axis perpendicular to the sediment water interface.

2.5. Sediment grain size

Grain size was determined from core samples collected in 2005 at FURG using standard pipette and sieve analysis (Lambe, 1951) and from grab samples in 2006 at NRL-SSC (QUE samples) using standard sieve analysis for the sand-sized fraction and a Micromeritics SediGraph III 5120 Particle Size Analyzer for the silt and clay-sized fraction ($< 64 \mu m$). The Micromeritics instrument determines grain size by determinations of X-ray attenuation across the path of the fluid column within which the homogeneously dispersed sediment is allowed to settle. Grain size was not determined from the 2007 samples.

2.6. Radioisotope geochronology—sediment accumulation rates

Geochronology was determined by analysis of samples taken from diver-collected sediment cores. During the 2005 cruise, diver-collected cores from 14 and 15 m water depths were subsampled by syringe at 5 cm intervals. The 14 m site was located along the Querência Transect in the primary depositional area and the 15 m site was located to the south of the transect through the depositional area. These samples are used to determine sediment accumulation rates in this area. During the 2006 cruise, divers collected sediment cores at two stations along the Querência transect, Que1 ($z = 7.9 m$) and Que14 ($z = 7.7 m$), for geochronological analysis to determine both sediment accumulation rates and sediment mixing rates. These cores were subsectioned at 1 cm intervals. Upon return to the laboratory, sediment samples were freeze-dried in a LABCONCO (Freezone-6) System after determining wet weights, ground and sealed in 70-mm-diameter Petri dishes. Porosities were calculated from water content (wet-dry weight) while assuming a particle bulk density of $2.65 g/cm^3$, value in agreement with results based on pycnometer tests (Dias and Alves, 2007). Samples were immediately counted for 1–2 days each using a Canberra low-energy intrinsic germanium gamma spectrometer, which has a 2000 mm² planar surface area. This initial count was used to calculate activities the short-period radiotracer ^{7}Be (53 d half-life), based upon the 455 keV photopeak. Samples were also recounted 21 days later (minimal time) to allow ^{210}Pb activities to achieve to secular equilibrium. ^{137}Cs activities were determined from this second count using the 661.6 keV photopeak. Total ^{210}Pb activity was determined from the 46 keV photopeak and supported ^{210}Pb activities were determined by using averaged activities of the ^{226}Ra daughters ^{214}Pb (295 and 352 keV) and ^{214}Bi (609 keV). Detector efficiencies for this geometry were calculated using a natural sediment standard (IAEA-300 Baltic Sea sediment) and detector backgrounds were determined using Petri blanks at the energies of interest.

3. Results

3.1. Grain size

Sediments obtained in cores collected were typically physically mixed with laminations of mud and sand displaying either fairly homogeneous stratigraphic layers or disrupted layers that depict physical mixing. Along the Querência Transect, sediments were

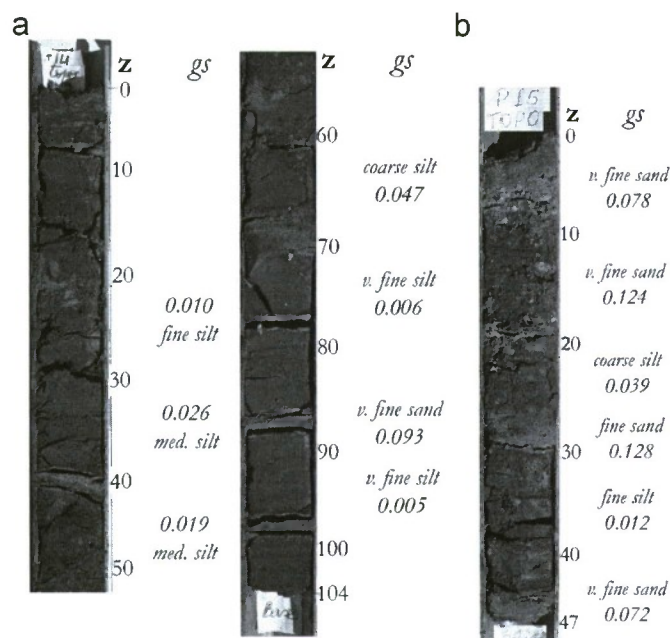


Fig. 4. (a) Sediment cores collected in the area of the mud depocenter display distinct features, such as physical mixing (pronounced at 20 cm below the seafloor) and layers of fine sand (light gray), which are interbedded in layers of mud (fine to coarse silt). In the lower portion of the core, numerous 1–2-cm-thick sand layers were deposited on mud layers that are ~9 cm thick. Depth below seafloor (z) is in cm and mean grain size (gs) is in mm. This core is 104 cm long. Grain size was not determined at all intervals. (b) Mean grain size (gs) for this core that was collected south of the mud depocenter is primarily sand with an interval of coarse and an interval of fine silt. This core is 47 cm long. Note: The transition from sand to silt occurs at 0.064 mm so if the mean grain size (gs) is below this value the sediment is a mud.

typically mud, with finer laminations of sand, whereas south of this transect, sandy deposits were more prevalent. The mean grain size for the muds at 14 m was typically in the range of fine to coarse silt (Fig. 4).

Surficial sediment samples displayed grain size ranging from clay to sand along the length of the Querência Transect with concentrations of sand increasing as distance from shore increased. A fairly abrupt change in grain size occurred from the 15 m depth, which classifies as clay-sized sediment and contained 9.5% sand to the 17.5 m depth, which classifies as a sand-sized sediment and contained 73.5% sand with sand concentrations increasing to 98% at the 29 m depth. Surficial sediments in water depths from 7 to 15 m are classified as clay, silty clay, or sandy clay. Sandy sediments dominated the sediment bed at some point inshore of the 7 m depth, perhaps at 6 m depth or slightly shallower (Table 1; Fig. 5).

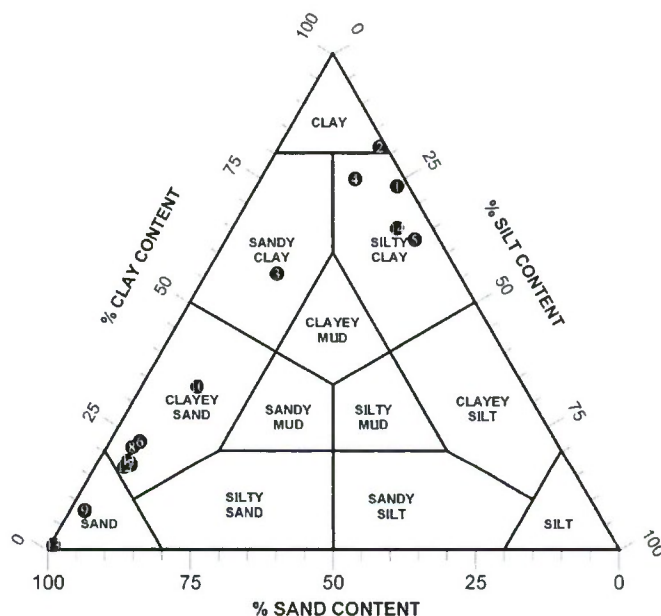


Fig. 5. The Shepherd plot of grain sizes for surficial sediments along the Querência Transect (2006) with sand concentration increasing seaward.

Table 1
The Querência Transect samples were collected in depths ranging from 7 to 29 m.

z (m)	Weight % by size class				W_n % dry	ρ (g/cm ³)	Lat. (South)	Long. (West)	Site#
	Gravel	Sand	Silt	Clay					
7.0	–	1.83	17.04	81.13	219	1.27	32°14.00'	52°10.99'	2
7.7	–	10.6	24.62	64.78	138	1.33	32°14.16'	52°10.84'	14
7.9	–	2	24.74	73.26	194	1.28	32°14.57'	52°10.24'	1
9.0	–	34.48	9.82	55.70	161	1.34	32°13.14'	52°11.36'	3
12.0	–	9.29	15.97	74.74	223	1.26	32°16.78'	52°8.28'	4
15.0	–	9.51	27.97	62.52	156	1.36	32°18.50'	52°6.25'	5
17.5	1.59	73.49	3.48	21.45	69.7	1.60	32°19.48'	52°4.63'	6
19.2	4.49	75.40	4.00	16.11	52.7	1.66	32°20.58'	52°3.32'	7
20.9	10.58	68.24	3.09	18.09	47.8	1.76	32°22.76'	52°0.93'	8
21.5	20.05	72.82	1.2	5.92	ND	ND	32°24.17'	51°59.05'	9
22.5	0.07	59.82	7.25	32.87	31.3	1.44	32°25.23'	51°58.21'	10
24.5	2.63	76.16	3.74	17.46	49.2	1.78	32°25.87'	51°55.47'	11
27.0	0.24	79.46	3.73	16.57	44.0	1.78	32°32.66'	51°47.51'	12
28.9	0.10	98.68	0.33	0.88	25.7	2.00	32°15.97'	51°11.81'	13

Clay and mud sediments are prevalent to 15 m depth, after which there is a distinct transition to sand sediment in deeper depths that initiates at 17.5 m depth. Water content (W_n) is indicative of in situ sediment density, grain size and sediment classification. z is depth below sea level in meters, ρ is density, W_n is water content on a dry grain density basis.

Table 2

Sediment behavior and rheological properties for mud samples collected along the Querência Transect in 2006.

	Initial yield (Pa)	Bingham yield (Pa)	Density (g/cm ³)
For density range of 1.05–1.10 g/cm ³			
Mean	0.78	1.26	1.08
SD	0.18	0.65	0.03
CoV	0.23	0.51	0.02
n	7	7	7
For density range of 1.10–1.15 g/cm ³			
Mean	1.35	3.16	1.15
SD	0.47	1.03	0.08
CoV	0.34	0.33	0.07
n	18	18	18
For density range of 1.15–1.20 g/cm ³			
Mean	1.45	4.36	1.17
SD	0.59	1.82	0.01
CoV	0.40	0.42	0.01
n	17	17	17
For density range of 1.20–1.30 g/cm ³			
Mean	2.75	11.37	1.26
SD	1.23	8.35	0.02
CoV	0.45	0.73	0.01
n	3	3	3

Values for the mean, 1 standard deviation (SD), Coefficient of Variation (CoV) and sample number (n) are provided for the initial yield, Bingham yield and density within each density range.

3.2. Rheology

Rheological evaluations performed on low-density mud samples (1.05–1.30 g/cm³) from the Querência Transect provide data on the initial yield stress (the first movement of the mud in response to an applied stress), the Bingham Yield stress (the stress that is extrapolated from the straight-line portion of the stress–strain curve to the stress axis) and the apparent viscosity (the ratio of stress to strain).

3.2.1. Initial (static) yield

Initial yields generally increased with increasing density. Fluid muds with densities ranging from 1.05 to 1.10 g/cm³ had average initial yields ranging 0.78 ± 0.18 Pa whereas fluid muds with densities ranging from 1.20 to 1.30 g/cm³ had average initial yields ranging from 2.75 ± 1.23 Pa (Table 2). Fig. 6a shows the density–initial yield stress relationships for all samples so qualified and indicates that there is a poor correlation between initial yield and density ($R^2 = 0.30$). The reasons that this correlation is poor may be related to differences in unmeasured constituents of the mud, such as organic matter (i.e., polymers, surfactants), cation exchange capacity, etc. that aids, indicates or increases cohesiveness of clay particles.

3.2.2. Bingham yield

Bingham yield stress typically increased with increasing density. The low-density fluid muds ranging from 1.05 to 1.10 g/cm³ had average initial yields of 1.26 ± 0.65 Pa whereas fluid muds with densities ranging from 1.20 to 1.30 g/cm³ had average initial yields of 11.37 ± 8.35 Pa (Table 2). Fig. 6b shows that the Bingham yield stress is poorly correlated with sediment bulk density ($R^2 = 0.38$), which may be for the same reason as the initial yield also provides a poor correlation.

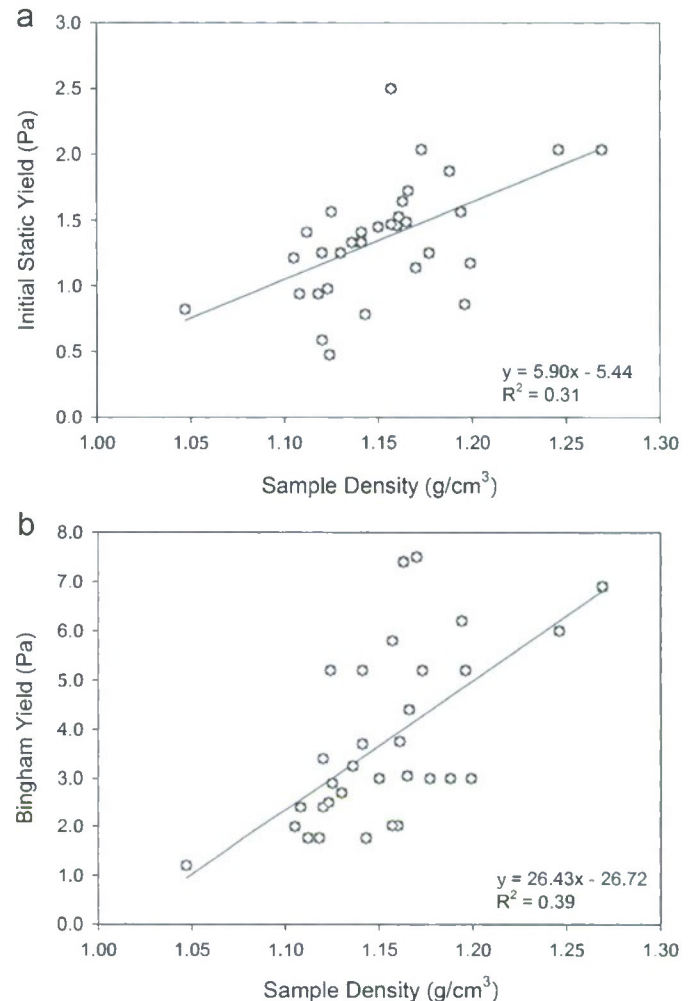


Fig. 6. Initial (a) and Bingham (b) yields for the Querência samples display poor linear correlations with sample density, but slightly better non-linear correlations with density.

3.2.3. Apparent viscosity

Apparent viscosities ranged from 4.72 to 0.02 Pa.s, with an average of 2.30 Pa.s, standard deviation of 0.97, and coefficient of variation of 42%. Suspension densities ranged from 1.05 to 1.269 g/cm³ with an average density of 1.151 g/cm³, a standard deviation of 0.042 and a coefficient of variation of 3.6%. Apparent viscosity profiles are displayed for samples of varying densities (from 1.047 to 1.296 g/cm³) (Fig. 7). All the profiles are similar and range from 0.78 to ~3.8 Pa.s. Behavior ranges from near Newtonian flow (low-shear rate Newtonian plateau) to shear thinning, with a tendency toward Newtonian at the highest shear rate (higher rpm needed to generate the high-shear rate Newtonian plateau). The lowest density sample shows a reduced low-shear rate Newtonian flow followed by only shear thinning through the highest shear rate, which is the 100 rpm bob rotation.

3.2.4. Atterberg limits

Querência samples are comparable to samples collected and analyzed by Dias and Alves (2007). A plasticity chart contains data from the Querência samples, which were collected in 2006, and from a 2004 sampling cruise that was conducted in the adjacent area (Dias and Alves, 2007; Fig. 8). Six Querência samples and eleven of the 2004 samples are classified as "inorganic clays of

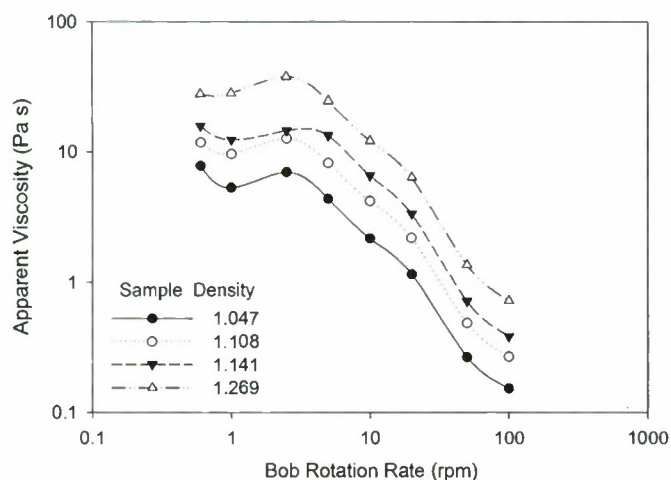


Fig. 7. The fluid mud response of the Querência samples is shear thinning through the range of densities that correspond to fluid mud. This decrease in apparent viscosity with increasing shear rate is realized after the initial yield is exceeded and the sediment has been deformed. The reason for the dip in apparent viscosity that occurs systematically for all densities is unclear.

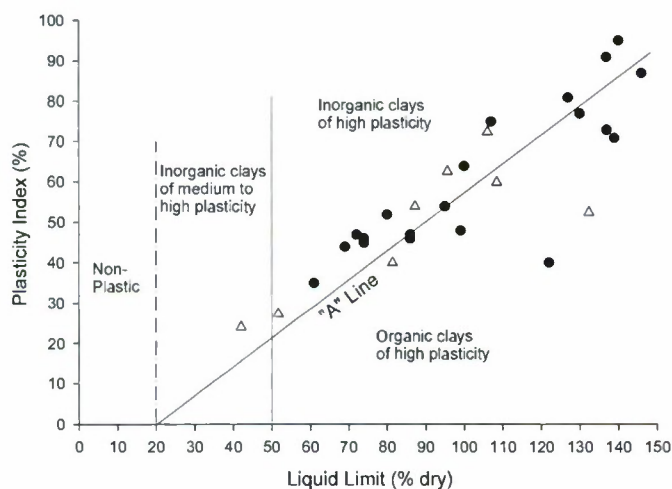


Fig. 8. Sediments from the Querência transect plot in the same location as those from previous surveys made in 2004 (triangles are from data provided by Dias and Alves, 2007) on the Cassagrande Chart depicted here. The sediments are classified as organic or inorganic clays of high plasticity in all but one case.

high plasticity", while three Querência and nine of the 2004 samples fall just below the A-line and are classified as "organic clays of high plasticity". One Querência sample was classed as "medium to high plasticity". Several other Querência samples had been collected but were determined to be non-plastic, such as occurs for samples collected from the sites that are deeper than 15 m depth (i.e., 17.5–27 m depths); these samples contained large amounts of sand, which is not the focus of this work and, therefore, they were not included on the plasticity chart.

3.3. Bearing strength and shear strength

Bearing strength determined from STING MKII penetrometer deployments correlated with surficial sediment sizes, especially in the shallower depths where the mud appears to have been continuous with depth below the sediment surface. Bearing strength increased seaward of the 15 m isobath with increasing sand concentrations. The lowest bearing strength recorded was at site 1 in 7 m water depth and this was determined to obtain a

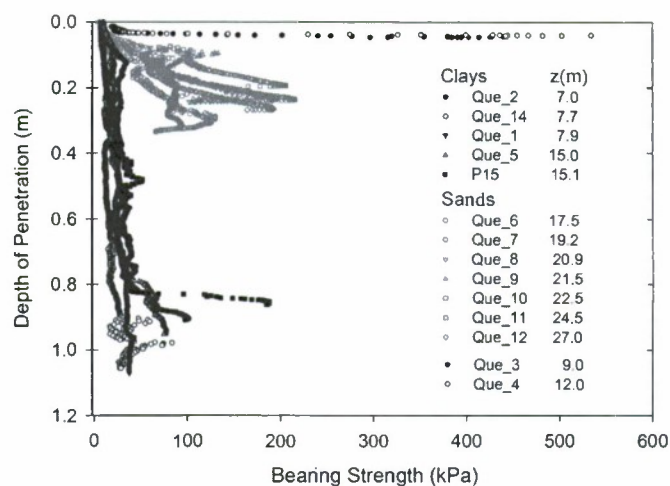


Fig. 9. Bearing strength determined for the muddy sediments of the Querência Transect (2006) were determined from penetrometer data. Two basic classes exist: (1) muddy sediments (blue lines) have lower bearing strength and allow greater penetration by the penetrometer, and (2) sand sediments (red lines) have higher bearing strength and lower penetration. Sites 3 and 4 display extremely stable sediments of high strength. (For interpretation of the references to colour in this figure legend, the reader is referred to the web version of this article.)

maximum value of 53 kPa at a depth of 1.06 m (Fig. 9). Bearing strength at site 12, a sand site located in 27 m water depth was determined to have a maximum bearing strength of 191 kPa. The sites with sandy surficial sediments had higher bearing strengths in the near surface, whereas the sites with surficial mud sediments, excluding those at sites 3 and 4, displayed significantly lower bearing strengths at all depths. The bearing strength profile obtained at the location of the 15 m deep site, which was occupied in 2005, it is typical of the muddy sediments in this area. In the upper portion of the sediments, a low bearing strength was determined, and at the base of the profile (~0.84 m), the bearing strength increases significantly, probably due to the presence of a thick sand layer or sand bed. Anomalous high bearing strengths, 554 and 533 kPa, occurred at sites 3 and 4, which were in 9.0 and 12.0 m of water, respectively. At these sites, penetration ceased within 5 cm of the sediment–water interface, suggesting a very dense layer of sediment just below the surface. Site 3 had a fairly large concentration of sand, 34.5%, in the surface grab sample (Table 1; Fig. 5). The bearing strength at each of these two sites was more than 2.5 times the bearing strengths at any of the other sites, which suggests that below the surficial mud layer, a dense layer of sand was present; unfortunately no core samples were taken at these locations.

Horizontal shear strength was determined directly from vane measurements and indirectly it was predicted from bearing strength using correlations established for this site. This correlation is in agreement with correlations thus established for areas with similar sediment (i.e., soft mud); in those cases, horizontal shear strength as determined by vane shear was found to be 1/10th of the recorded bearing strength (Abelev, 2008; Preston et al., 1999). Shear strength indicates the amount of shear that must be imparted on sediment to cause it to fracture, deform or liquefy. Shear strength values were predicted to range from 1.2 for surficial muds to 11 kPa at the depth of penetration in areas that contained mud sediments in the surface (i.e., QUE 1, 2, 5, 14, and P15) and continuously low bearing strengths to greater than 40 cmbsf. The maximum shear strength values for sites QUE 1, 2, 5 and 14 was 3.6 kPa just above the complete penetrometer penetration depth. Rapid increase in strength just below this value indicates the potential for sandy basal layer. This value is approximately ~350 times greater than the Bingham yield

stress of remixed mud determined from rheological measurements (Fig. 10).

3.4. Geochronology

In samples evaluated from cores collected in 2005, the presence of ^{137}Cs (activities $<0.25\text{ dpm/g}$) to the base of the 14 m site (62 cm) located at 32.227°S , 52.188°W , suggests this entire interval was deposited after the onset of thermonuclear bomb testing (1954–1956). Downcore ^{210}Pb at this site (Fig. 11a) shows the presence of a surface mixed layer (SML) of homo-

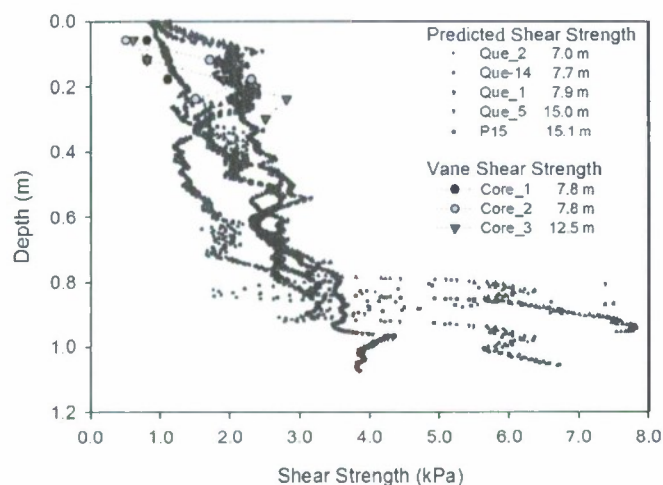


Fig. 10. In the mud samples, predicted horizontal shear strengths (1/10th the bearing strength) fall within the same range as shear strengths determined from vane shear measurements on diver-collected cores. The predicted horizontal shear strengths increase slowly with depth to the base of the penetration depth, which is believed to be the sandy basal deposit.

geneous excess activity ($\sim 3\text{ dpm/g}$) with exponential decay below this depth. ^7Be exhibits homogenous activities ($\sim 0.7\text{ dpm/g}$) in the upper 12 cm of the SML, suggesting this interval was mixed within the last $\sim 250\text{ d}$ (4–5 half-lives). Given that the thickness of the SML exceeds the depth ($<10\text{ cm}$) of typical biological down mixing of ^{210}Pb in coastal marine environments, this suggests that physical mixing (erosion and redeposition) has emplaced the upper section of this profile (Kuehl et al., 1995). ^{210}Pb sediment accumulation rate calculation of the exponential section of the profile (Fig. 11a) at the 14 m site ($r^2 = 0.98$) yields $0.49 \pm 0.09\text{ cm/y}$. Cores from the 15 m site (32.419°S , 52.210°W) show little or no SML or ^7Be activity and an exponential decrease in ^{210}Pb activity from the sediment surface, indicating less intense physical mixing and limited recent ($<250\text{ d}$) sediment deposition. ^{137}Cs is only present to about 20 cm, coincident with the depth limit of excess ^{210}Pb . Decadal-scale sediment accumulation at this site from ^{210}Pb is $0.25 \pm 0.02\text{ cm/y}$ ($r^2 = 0.91$).

Geochronological analysis on cores collected from the QUE1, the 7.9 m site, in 2006 at 1 cm depth intervals shows distinct differences from the 2005 sites. In both cores, Cs is present at similar activities to 2005 to the core bottom (24 cm in the QUE 1 core and 11 cm in QUE14 core). However, ^{210}Pb the QUE1 core (Fig. 11b) exhibits four layers rather than a single SML and exponential trends: two layers of relatively high excess ^{210}Pb activity (6–7 dpm/g) at 0–6 and 10–20 cm, separated by low activity zones (4–6 dpm/g). ^7Be activity is also found in some intervals at high activities (up to 10 dpm/g) and is not present in other intervals. Similar trends are observable in the shorter QUE14 core, 7.7 m site, which has a similar pattern of high excess ^{210}Pb activity at 0–2 and again below 9 cm depth, with ^7Be occurrence in the lower zone of high Pb activity. These layers are likely associated with variability in mineralogy and grain size, that is the high ^{210}Pb and ^7Be activity typically coincides with higher contents of clay, which preferentially adsorb these radiotracers. This is also observable in the Ra-supported ^{210}Pb levels (Fig. 11b), which are lower in the coarser intervals. However, the high Be in

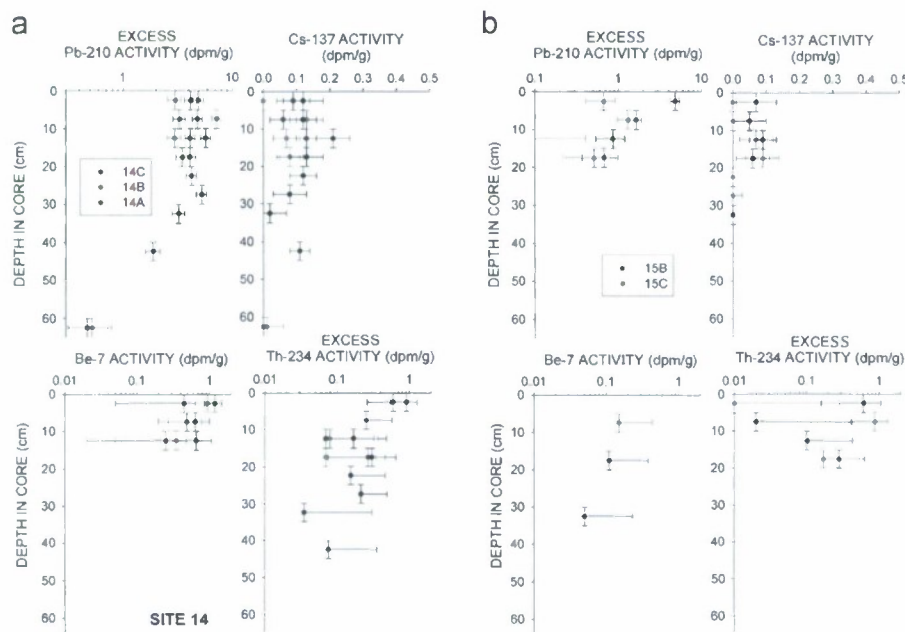


Fig. 11. (a) Geochronology from 14 m water depth site in 2005. The diver cores shows excess ^{210}Pb surface mixed layer in the upper 30 cm and exponential decay to the base of the core (left graph). ^7Be in this core (right graph) is homogenous and limited to the upper 12 cm (above dotted line). (b) Geochronology of the P15 diver core collected in 2005 (left graph) showing downcore variable excess ^{210}Pb activity that coincides with changes in supported ^{210}Pb activity (open triangles). ^7Be (right graph) is also highly variable, with intervals with no Be activity marked by a thick horizontal line.

some of these zones may also indicate two other possibilities: (1) there is a fresh or more continental (estuarine or lagoonal derived) source for the material, or (2) there is a down-stream effect, that is this sample site is farther from the source material.

4. Discussion and summary

This evaluation characterizes the sediment deposit adjacent to and along the instrumented transect from Querência seaward, adjacent to Cassino Beach by quantifying physical and geotechnical properties and the areal extent of a previously characterized mud deposit (Calliari and Fachin, 1993). As Winterwerp et al. (2007) indicates, the most important properties of the mud in the context of water-wave dampening are the areal extent and thickness of the mud deposit, the mud response to shear stress and the mud density. This data then provides requisite input for numerical models of wave energy dissipation used for this site (Rogers and Holland, this issue). Therefore, sample transects were established, in situ measurements were made and mud was analyzed to determine the areal extent and thickness of the mud as well as the shear strength, viscosity and density of the mud.

The mud deposit through which the Querência Transect passed is bounded by sand deposits to the east, west and south and the Patos Lagoon jetty to the north. Initially, suspended sediment is transported out of the lagoon mouth in a SSE direction ($\sim 163^\circ$) after which the sediment is transported cyclonically westward towards the beach and then northerly towards the jetty (Vinzon et al., this issue, Fig. 12). Due to gravitational effects, these sediments are sequestered such that sandy sediments are deposited southeast of the lagoon mouth to become nearly pure sand offshore (79.5% sand at 27 m water depth and 98% sand in 28.9 m water depth) and mud is transported to the west of this lagoon mouth trend (SSE or $\sim 163^\circ$). The mud that is transported to the accumulation zone in the ~ 6 –15 m water depths rapidly accumulates on the seafloor as determined from geochronological data. These locally sourced muds accumulate rapidly with up to 50 mm/yr possible as determined from Pb^{210} data. Inshore of ~ 6 m water depth, sand sediments dominate in the high-energy nearshore and on to the beach (Figs. 1 and 4). To the south of the Querência Transect and the mud deposit (site P15; Fig. 1) the sediments become sandy. At the base of the mud, sand sediments dominate (Calliari, 2006). Therefore, the sand deposits provide approximate boundaries of the mud deposit, which is ~ 9 km long and up to 28 km wide, that is the distance from the jetty to site P15 (Fig. 1). The thickness of the mud deposit, along the Querência Transect, ranges from <1 to ~ 2 m, as determined by penetrometer insertion depths, diver cores, and echosounder data (Holland et al., 2007; Calliari and Fachin, 1993; Fig. 9).

Shear strength of this mud deposit was evaluated in situ using a penetrometer (Fig. 3) and in the laboratory using a shear vane on diver-collected cores. It is important to note that these devices evaluate different shear properties of the mud. Specifically, the penetrometer quantifies normal incidence shear strength and the shear vane quantifies horizontal shear strength. Normal incidence shear strength was correlated for these sediments to be ten times the horizontal shear strength determined on diver-collected cores, which is in keeping with previous determinations (Preston et al., 1999) and this correlation appears to fit the data pretty well (Fig. 10). The importance of establishing a correlation is that diver cores were not obtained everywhere because sediment thickness was greater than the length of the diver cores or because collection was prohibited by logistical constraints (i.e., rough seas, limited light, lack of dive time). Within diver cores that were evaluated, the horizontal shear strengths ranged from 0.6 at 6 cm

below the seafloor to 2.8 kPa at 30 cm below the seafloor, which is the depth to which diver cores sampled. Horizontal shear strengths display a slightly wider range than the normal incidence shear strengths (determined by penetrometer), which ranged from 1.2 to 2.6 kPa in the upper 30 cm of the mud deposit. Below the 30 cm depth, normal incidence shear strength data obtained with the penetrometer becomes quite useful. From these normal incidence shear strength determinations, the horizontal shear strength was predicted to range from 1.2 to 3.6 kPa through the thickness of the mud deposit, which was up to 1.4 m. Near the maximum depth of penetration, the normal incidence shear strength increased rapidly probably due to a highly resistant layer, such as a basal sand layer. These shear strengths fall within the range of shear strengths determined from surficial, low-density muds from the Kerala Coast of India, the Bearing Sea, Galveston Bay, USA and the Atchafalaya Basin, Northern Gulf of Mexico, which were determined to range from 0.5 to 4 kPa (Silva et al., 1996; Narayana et al., 2008).

The low shear strength at depth within the mud may be attributable to rapid sediment accumulation, which tends to inhibit sediment dewatering, compaction and grain–grain interactions. Accumulation rates of 25 mm/yr at the southern portion of the depocenter (site P15; green box at 15 m in Fig. 1) and 50 mm/yr (site 14; red box at 14 m Fig. 1) were determined. Similar accumulation rates have been determined at an adjacent site, near Cassino Beach, and are comparable to rates determined on muddy inner shelves proximal to the Amazon (Kuehl et al., 1986), Mississippi (Corbett et al., 2006), Atchafalaya (Neill and Allison, 2005) and Ganges-Brahmaputra (Kuehl et al., 1997) rivers. Therefore, rapid accumulation and associated processes may play an important role in establishing and maintaining low sediment strength at this site to the 80 cmbsf to which low strength occurs. However, additional forces that increase pore pressures and inhibit consolidation, such as wave loading and basal fluid flow may also work to maintain low strength deep by increasing pore pressures within this mud deposit.

Sediments that are resuspended from the deposit or recently settled from the entrained deposit have lower sediment strengths when evaluated by viscometer. To address the strength and behavior of sediments that are remixed or recently settled, rheological determinations of sediment behavior and viscosity were made for muds that had density in the range 1.05–1.30 g/cm³. Remixed surficial muds were analyzed using a Couette strain-controlled viscometer, the Brookfield RVT. Values of stress and the applied stress rate (bob rotation rate) were determined according to Brookfield's recommendations and then corrected using a modified form of the Maron and Krieger (1954) equations as suggested by Rosen (1979). This approach was chosen because the Maron and Krieger (1954) formulation does not assume a specific rheological behavior and has been found to agree with other formulations, such as that of Worrell–Tuliani (Toorman, 1994). Most important to our determinations is that this correction ensures that the shear rate at the bob surface, the portion of the viscometer that is acting upon the mud and from which strain calculations are made, was accurate and free from artifacts, such as slippage (Barnes, 1999). During these measurements, an initial yield and a Bingham yield stress were determined within sediments that were mixed to have a densities ranging from 1.05 to 1.30 g/cm³. The initial (static) yield that occurs during the first applied strain ranged from 0.59 to 2.6 Pa through this density range. During these evaluations, the mud continued to deform and was followed by a second yield, the Bingham yield stress, which ranged from 1.26 to 11.37 Pa through this density range. In general, the yield strength increased with increasing density, but poor correlations between strength and density indicate that the sediment behavior is controlled by

factors, which may be due to variability in mineralogy, organic matter content and type, or grain size distribution. For all samples, flow behavior indicates that the maximum viscosity exists over the range of the first few shear rates, which correspond to the initial yield stress and the Bingham yield stress. The occurrence of two yields in a single sample has been noted to occur in other mud samples and when this occurs, the mud is characterized as a non-ideal Bingham fluid (Nguyen and Boger, 1992; Toorman, 1994). After the Bingham yield stress exceeded, the mud behaved more like a Bingham fluid, where the ratio of shear stress to shear rate became more linear. Therefore, this mud may also be characterized as a viscoplastic material that does not return to its initial state after the initial yield is exceeded (Barnes, 1999). Based on Atterberg limits that were made previously on muds in this area, the sediment behavior remains comparable through the period of these evaluations, that is 2004–2007 (Dias and Alves, 2007).

This study indicates that there is a large supply of soft mud captured in the area of the Querência Transect, however the amount of mud that can be resuspended, liquefied, and transported as a fluid depends upon many factors that were not measured and which are not readily measurable, such as the applied stresses due to waves and currents, the sediment pore pressure, the temporal history of the stress, and the thickness of the fluid mud. It is recommended that further work should be undertaken to establish clear methods and guidelines to accurately determine the fluid mud volumes, the behavior of this mud, and the inherent properties, constituents and mineralogy of the mud that may control local variability by simultaneously employing a variety of techniques (e.g., acoustics, Densitune, penetrometers, in situ shear measurements techniques, piezometers, etc.) as suggested by McAnally et al. (2007).

5. Conclusions

1. The mud deposit along the Querência Transect is confined by sand deposits in the beach and nearshore, the offshore and the south and the rock jetty that bounds the southern portion of the lagoon mouth. The mud is concentrated in a relatively shallow area in approximately 6–15 m depth which lies along a transect that is approximately 9 km long and may extend 28 km from north to south. Soft mud is at least 0.85–1.25 m thick, in some locations, along the Querência Transect.
2. Sediment accumulation rates in the vicinity of the “depocenter” are quite high, 50 mm/yr, and comparable to those in the Amazon Delta, Atchafalaya Basin, the Mississippi River and the Ganges-Brahmaputra River. The highest accumulation rates, that we determined, are found along the 14 m isobath, along the instrumented transect that was set up 2005, in an area that is dominated by mud deposition. Accumulation rates remain high at the southern portion of this area.
3. The sediments in the muddy area adjacent to the depocenter (and Querência) display horizontal shear strengths typical of fine grained marine sediments, such as those along the Kerala Coast, the Gulf of Mexico, and the Bearing Sea.
4. The mud is a non-Newtonian fluid; it possesses both an initial (static) yield stress and a Bingham yield stress and therefore behaves as a non-ideal Bingham fluid. Between these two yield stresses the sediment exhibits its highest viscosity. After the Bingham yield stress, the viscosity declines, therefore this mud is classified as a shear thinning fluid.
5. The low shear strength of the reconstituted and fully remixed muds is similar to those of surficial marine sediments. They are typically 2–3 orders of magnitude lower than the horizontal shear stress values measured on undisturbed sediments, which

were collected by SCUBA divers and analyzed with a shear vane.

Acknowledgements

We thank Susana Vinzon for overseeing this project. We owe thanks for USM, FURG, Tulane and NRL personnel who enabled this work to be completed, especially Dan Duncan at TU for performing geochronological analysis, Evan Dillon for performing grain size analysis at NRL, geological technicians at FURG, the divers in Susana's lab and the Pedro de Souza Pereira, Rafael Guedes (diving) and Renato Espirito-Santo at FURG. Additional gratitude goes to Cassino 8 and the *R/V Larus* captains and crews. C. Brunner and USM provided lab space to perform rheological work. We thank the Office of Naval Research for base funding to the Naval Research Laboratory and for funding the experiment and collaborators directly. This is Program Element number 0601153N.

References

- Allison, M.A., Lee, M.T., 2004. Sediment exchange between Amazon mudbanks and shore-fringing mangroves in French Guiana. *Marine Geology* 208, 169–190.
- Allison, M.A., Kineke, G.C., Gordon, E.S., Goñi, M.A., 2000. Development and reworking of a seasonal flood deposit on the inner continental shelf off the Atchafalaya River. *Continental Shelf Research* 20 (16), 2267–2294.
- Barnes, H.A., 1999. The yield stress – a review or ‘πανταροί’ – everything flows? *Journal of Non-Newtonian Fluid Mechanics* 81, 133–178.
- Calliari, L.J., personal communication, 2006.
- Calliari, L.J., Fachin, S., 1993. Laguna dos Patos. Influência nos depósitos lamíticos costeiros. *Pesquisas* 20 (1), 57–69.
- Corbett, D.R., McKee, B.A., Allison, M.A., 2006. Nature of decadal-scale sediment accumulation in the Mississippi River deltaic region. *Continental Shelf Research* 26, 2125–2140.
- Dalrymple, R.A., Liu, P.L.-F., 1978. Waves over soft muds: a two layer model. *Journal of Physical Oceanography* 8, 1121–1131.
- Dias, C., Alves, A., 2007. Geotechnical Properties of the Cassino Beach Mud (submitted to this issue).
- Fan, S., Swift, D.J.P., Traykovski, P., Bentley, S., Borgeld, J.C., Reed, C.W., Niedoroda, A.W., 2004. River flooding, storm resuspension, and event stratigraphy on the northern California shelf: observations compared with simulations. *Marine Geology* 1–4, 17–41.
- Faas, R.W., 1991. Rheological boundaries of the mud: where are the limits? *Geo-Marine Letters* 11, 143–146.
- Faas, R.W., 1995. Mudbanks of the southwest coast of India III: role of non-Newtonian flow properties in the generation and maintenance of mudbanks. *Journal of Coastal Research* 11, 911–917.
- Feng, J., 1992. Laboratory experiments on cohesive soil bed fluidization by water waves. M.S. Thesis, University of Florida, Gainesville, p. 109.
- Fernandes, E.H.L., Dyer, K.R., Möller, O.O., Niencheski, L.F.H., 2002. The Patos lagoon hydrodynamics during and El Niño event (1998). *Continental Shelf Research* 22 (11–13), 1699–1713.
- Gabioy, M., Vinzon, S.B., Paiva, M.A., 2005. Tidal propagation over fluid mud layers on the Amazon shelf. *Continental Shelf Research* 25, 113–125.
- Gade, H.G., 1958. Effects of a non-rigid, impermeable bottom on plane surface waves in shallow water. *Journal of Marine Research* 16 (2), 61–82.
- Holland, K.T., Vinzon, S.B., Calliari, L.J., 2007. A field study of coastal dynamics on a muddy coast offshore of Cassino Beach, Brazil (submitted to this issue).
- Inglis, C.C., Allen, F.H., 1957. The regimen of the Thames Estuary as affected by currents, salinities and river flow. *Proceedings of the Institute of Civil Engineering* 7, 827–878.
- Isobe, M., Huynh, T.N., Watanabe, A., 1992. A study on mud mass transport under waves based on an empirical rheological model. In: *Proceeding of the 23rd Coastal Engineering Conference* 3, ASCE, New York, pp. 3093–3106.
- Jiang, F., Mehta, A.J., 1996. Mudbanks of the southwest coast of India V: wave attenuation. *Journal of Coastal Research* 12, 890–897.
- Krieger, I.M., Maron, S.H., 1954. Direct determination of flow curves for non-Newtonian fluids. III. Standardized treatment of flow curves. *Journal of Applied Physics* 25 (1), 72–75.
- Kuehl, S.A., Pacioni, T.D., Rine, J.M., 1995. Seabed dynamics of the inner Amazon shelf: temporal and spatial variability of surficial strata. *Marine Geology* 135, 283–302.
- Kuehl, S.A., Levy, B.M., Moore, W.S., Allison, M.A., 1997. Subaqueous delta of the Ganges-Brahmaputra river system. *Marine Geology* 144, 81–96.
- Kuehl, S.A., DeMaster, D.J., Nittrouer, C.A., 1986. Nature of sediment accumulation on the Amazon continental shelf. *Continental Shelf Research* 6, 209–226.
- Lambe, T.W., 1951. *Soil Testing for Engineers*. Wiley, New York, pp. 22–28.
- Maa, J.P.Y., Mehta, A.J., 1987. Mud erosion by waves: a laboratory study. *Continental Shelf Research* 7, 1269–1284.

- McAnally, W.H., Friedrichs, C., Hamilton, D., Hayter, E., Shreshtha, P., Rodriguez, H., Sheremet, A., Teeter, A., 2007. Management of fluid mud in estuaries, bays, and lakes. I: present state of understanding on character and behavior. *Journal of Hydraulic Engineering* 133 (1), 9–22.
- MacPherson, H., 1980. The attenuation of water waves over a non-rigid bed. *Journal of Fluid Mechanics* 97, 721–742.
- Mehta, A.J., 1989. On estuarine cohesive sediment suspension behavior. *Journal of Geophysical Research-Oceans* 94 (C10), 14303–14314.
- Mei, C.C., Liu, K.F., 1987. A Bingham plastic model for muddy sea bed under long waves. *Journal of Geophysical Research* 92 (C13), 14581–14594.
- Mitchell, J.K., 1976. *Fundamentals of Soil Behavior*. Wiley, New York, 442 pp.
- Mulhearn, P.J., 2003. Influences of penetrometer tip geometry on bearing strength estimates. *International Journal of Offshore and Polar Engineering* 13 (1), 73–78.
- Neill, C.F., Allison, M.A., 2005. Subaqueous deltaic formation on the Atchafalaya Shelf, Louisiana. *Marine Geology* 214, 411–430.
- Nguyen, Q.D., Boger, D.V., 1992. Measuring the flow properties of yield stress fluids. *Annual Review of Fluid Mechanics* 24, 47–88.
- Niencheski, L.F.H., Windom, H.L., Moore, W.S., Jahnke, R.A., 2007. Submarine groundwater discharge of nutrients to the ocean along a coastal lagoon barrier, Southern Brazil. *Marine Chemistry* 106 (3–4), 546–561.
- Narayana, A.C., Jago, C.F., Manojkumar, P., Tatavarti, R., 2008. Nearshore sediment characteristics and formation of mudbanks along the Kerala coast, southwest India. *Estuarine, Coastal and Shelf Science* 78, 341–352.
- Preston, J.M., Collins, W.T., Mosher, D.C., Poeckert, R.H., Kuwahara, Bennett, R.H., 1999. The strength of correlations between geotechnical variables and acoustic classifications. *Proceedings of the MTS/IEEE Oceans* 99, 1123–1128.
- Rosen, M.R., 1979. Characterization of non-Newtonian flow. *Polymer, Plastic Technology Engineering* 12 (1), 1–42.
- Sheremet, A., Mehta, A.J., Liu, B., Stone, G.W., 2005. Wave-sediment interaction on a muddy inner shelf during Hurricane Claudette. *Estuarine, Coastal and Shelf Science* 63, 225–233.
- Shibayama, T., Takikawa, H., Horikawa, K., 1986. Mud mass transport due to waves. *Coastal Engineering in Japan* 29, 151–161.
- Silva, A.J., Brandeis, H.G., Veyera, G.E., 1996. Geotechnical characterization of the surficial high-porosity sediments in Eckernforde Bay. *Geo-Marine Letters* 16, 167–174.
- Toorman, E.A., 1994. Analytical solution for the velocity and shear rate distribution of nonideal Bingham fluids in concentric cylinder viscometers. *Rheological Acta* 33 (3), 193–202.
- Tsuruya, H., Nakano, S., Takahama, J., 1987. Interactions between surface waves and a multi-layered mud bed. Report of the Port and Harbor Research Institute, Ministry of Transport, Japan 26 (5), 137–173.
- Vinzon, S.B., Winterwerp, J.C., de Boer, G.J., Nogueira, R., this issue. Mud deposit formation on the open coast of the larger Patos Lagoon–Cassino Beach system (this issue).
- Wells, J.T., Coleman, J.M., 1981. Physical processes and fine-grained sediment dynamics, coast of Surinam, South-America. *Journal of Sedimentary Petrology* 51 (4), 1053–1068.
- Williams, R.W., 1979. Determination of viscometric data from the Brookfield R.V.T. viscometer. *Rheological Acta* 18, 345–359.
- Winterwerp, J.C., de Graaff, R.F., Groeneweg, J., Luijendijk, A.P., 2007. Modeling of wave damping at Guyana mud coast. *Coastal Engineering* 54, 249–261.
- Wroth, C.P., Wood, D.M., 1978. Correlation of index properties with some basic engineering properties of soils. *Canadian Geotechnical Journal* 15 (2), 137–145.